# Redshifts of faint 3CR radio sources

M. A. C. Perryman\* Astronomy Division, Space Science Department of ESA, ESTEC, Noordwijk, The Netherlands

S. J. Lilly\* and M. S. Longair\* Royal Observatory, Blackford Hill Edinburgh EH9 3HJ, Scotland

A. J. B. Downes\* Mullard Radio Astronomy Observatory, Cavendish Laboratory, Madingley Road, Cambridge CB3 0HE

Received 1983 December 5; in original form 1983 October 24

Summary. Low-resolution optical spectra of nine faint objects associated with 3CR radio sources in the right ascension range 22–07 hr have resulted in the determination of seven new redshifts (4C 12.03, 3C 14, 22 and 41, 4C 14.11, 3C 441 and 457). One further redshift (3C 172) is provisional, but for the remaining object (3C 65) no redshift has been determined.

#### 1 Introduction

Since its construction, the sample of bright 3CR radio sources (Jenkins, Pooley & Riley 1977) has been the subject of intensive study at all accessible wavelengths. Laing, Riley & Longair (1983) have re-examined this complete sample, and using the selection criteria,  $S(178 \text{ MHz}) \ge 10 \text{ Jy}$ ,  $\delta \ge 10^{\circ}$ ,  $|b| \ge 10^{\circ}$ , have added several sources previously omitted because of their large angular extent. A few sources were also removed from the original sample. For the 173 sources in the revised sample, 162 have reliable optical identifications, while a further four have provisional identifications. This 3CR sample is unique amongst low-frequency radio surveys in the completeness of the optical identifications. While redshifts are known for almost all the quasars, however, there are still a number of faint galaxies that do not have measured redshifts (Laing et al. 1983, and references therein).

The task of obtaining spectroscopic redshifts for the remaining identifications is challenging since most of them are fainter than 20th magnitude. Recent work by Spinrad and his collaborators (Smith & Spinrad 1980a; Spinrad, Stauffer & Butcher 1981; Spinrad 1982) has resulted in a number of redshift determinations and has illustrated the observational difficulties involved. The remaining objects are likely to represent some of the most distant

<sup>\*</sup> Visiting Astronomer, Kitt Peak National Observatory, operated by the Association of Universities for Research in Astronomy, Inc., under contract with the National Science Foundation.

galaxies known, and the determination of their redshifts is important in providing further insight into the evolution of the radio source population and of the parent galaxies.

In this paper, we report spectroscopic observations of nine 3CR optical identifications with previously unknown redshifts; all such objects contained in the sample of Laing et al. (1983) within the right ascension range 22–07 hr were observed, except 3C 469.1. These nine objects include three sources recently incorporated into the 10-Jy complete sample, and one identification classified as a quasar on the basis of its optical morphology.

## 2 Observations and analysis

The observations were made on 1982 October 13–16 with the RC Spectrograph and the Cryogenic Camera at the Mayall 4-metre telescope of the Kitt Peak National Observatory (KPNO). The dispersive element was the grism numbered 770 in the KPNO system, with 300 lines per mm, providing an undeviated central wavelength of 5970 Å and a spectral coverage between 4500–7900 Å at a scale of 4.26 Å per pixel. A long slit of aperture 2.5 arcsec × 4.45 arcmin was used for all observations, resulting in a nominal spectral resolution of 15 Å FWHM and a scale of 0.84 arcsec per pixel along the slit.

The Cryogenic Camera employs a thinned  $800 \times 800$  pixel Texas Instruments charge-coupled device (CCD) array. The pixel size is  $15 \mu m$  square and the read-out noise was 8-10 electrons rms per pixel. The optical system illuminates the central  $350 \times 800$  pixels, the remaining area providing a measure of the electronic offset bias level and of the dark-current signal for each exposure. The CCD used was free from column defects over the active area, and had only a few bad pixels. Ripples in the thinned chip resulted in focus variations across the surface, particularly towards the long-wavelength edge. A more complete description of the instrument is given by De Veny (1982).

Table 1 lists the integration times used, approximate r magnitudes of the objects from the compilation by Laing et al. (1983) and the principal results of this programme. For the longest integrations, two or more exposures per field were taken to allow the identification and removal of cosmic ray events, and to minimize the effects of atmospheric field rotation and scale compression between the slit and the guide probe. For calibration, two or more quartz continuum exposures were taken using a colour-balancing filter for the flat-fielding of each exposure. Sky exposures were taken once per night to determine the relative throughput along the slit. Wavelength calibration was performed using a He-Ne-Ar exposure for each field; this exposure was also used to correct for the distortion caused by

Table 1.	Observatio	onal details a	nd principal results.
Object	r	Observing time (s)	<sup>z</sup> e

0bje	ect r	Observing time (s)	<sup>z</sup> e	<sup>z</sup> a	Rest wavelength coverage (A)	I	<sup>z</sup> pred
4C 12.	.03* 17	1000	0.156 <u>+</u> 0.001	0.157 <u>+</u> 0.001	3900-6850	. <del>.</del>	0.11
3C 14	20	3x3000	1.469 ± 0.001	-	1850-3200	-	1.0
3C 22	20.5	2000+3000	0.938 <u>+</u> 0.001	<del>-</del>	2300-4100	0.18	0.60
3C 41	21	2000	0.795 <u>+</u> 0.001	<del>-</del>	2500-4400	0.08	0.78
3C 65	23	2x3000	-	-	, <del>-</del>	-	2.0
4C 14.	.11* 19	900	-	0.206 ± 0.001	3750-6550	-	0.38
3C 172	20	2000	0.520 **	- *	2950-5200	0.3	0.52
3C 441	21	2000	0.708 <u>+</u> 0.001	-	2650-4600	0.32	0.78
3C 457	* 19.5	2x2000	0.428 <u>+</u> 0.001	-	3150-5550	0.75	0.31

<sup>\*</sup> additions to the original 10 Jy sample proposed by Laing et al.(1983)

<sup>\*\*</sup> redshift requiring confirmation

the camera optics. Observations of the standard stars Hiltner 102 and 600 were used to convert the resulting spectra to relative energy units using the calibrations by Stone (1977).

Preliminary reductions used the standard KPNO software. Batch programs (Scott, Hammond & Goad 1982) perform the background subtraction and flat-fielding. The long-slit analysis package RV (Goad 1982) was used with the Interactive Picture Processing System to determine the curvature correction and wavelength-dispersion solution for each image. A mean sky spectrum was constructed by averaging nearby rows of pixels that were free from other objects. The subsequent analysis of the spectra, including the determination of line centres and equivalent widths, was carried out with the SPICA package on the UK STARLINK network. Because of ripples in the chip surface, the spectra were de-focused at both the longest and shortest wavelengths and so they were extracted from the 2-dimensional

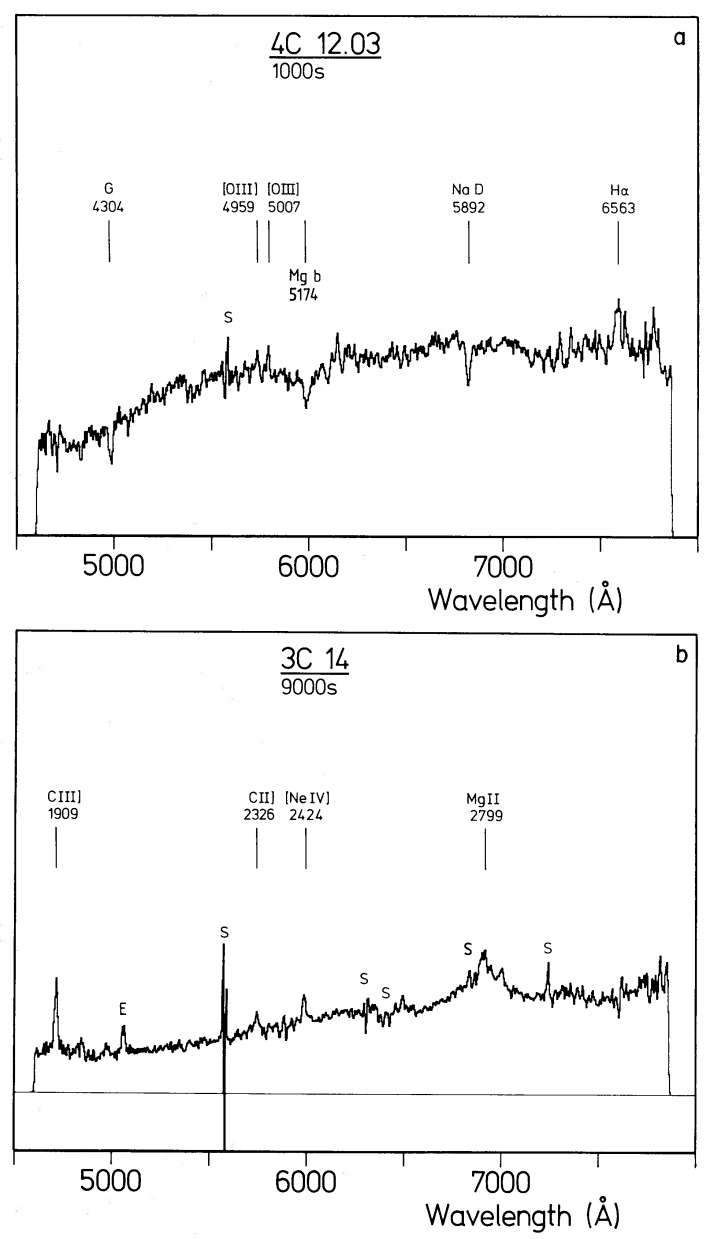


Figure 1. Reduced spectra of the nine objects in energy units per frequency interval on an arbitrary scale as a function of the observed wavelength. Identified emission and absorption lines, cosmic-ray-event features (E) and incomplete sky-subtraction features (S) are labelled. For comparison a typical night-sky spectrum is also presented.

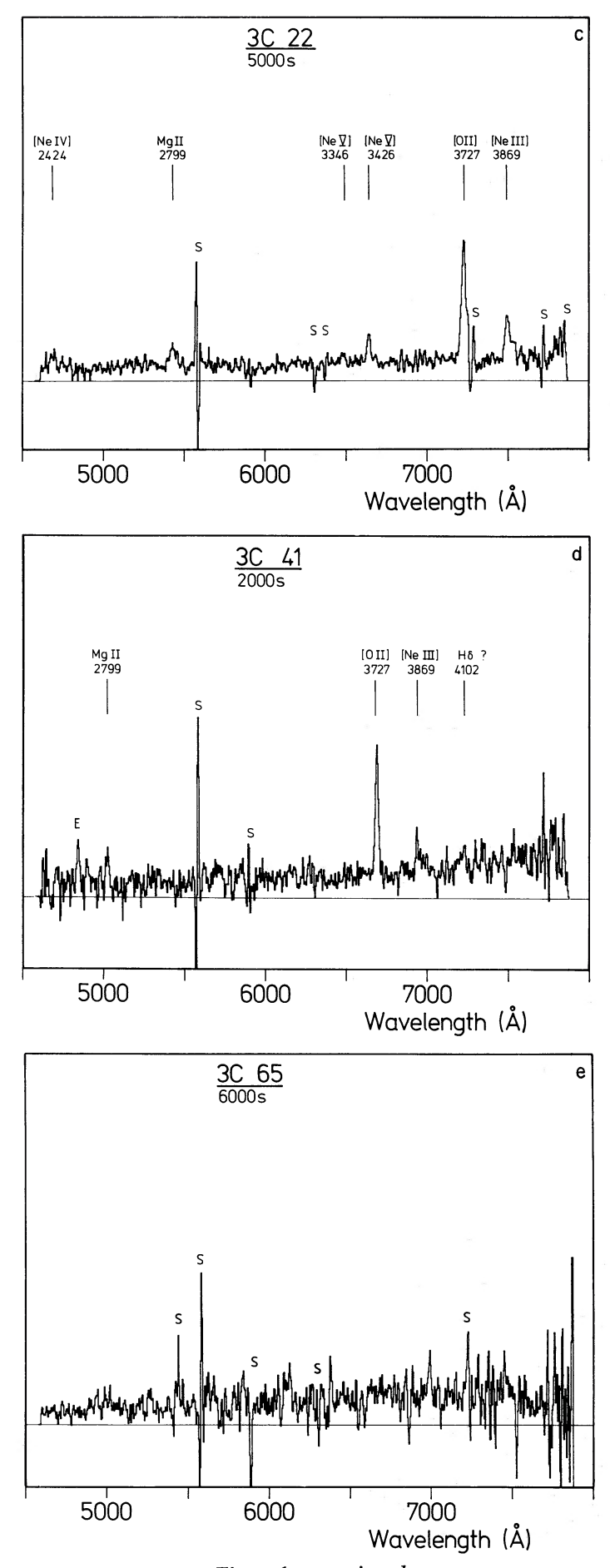
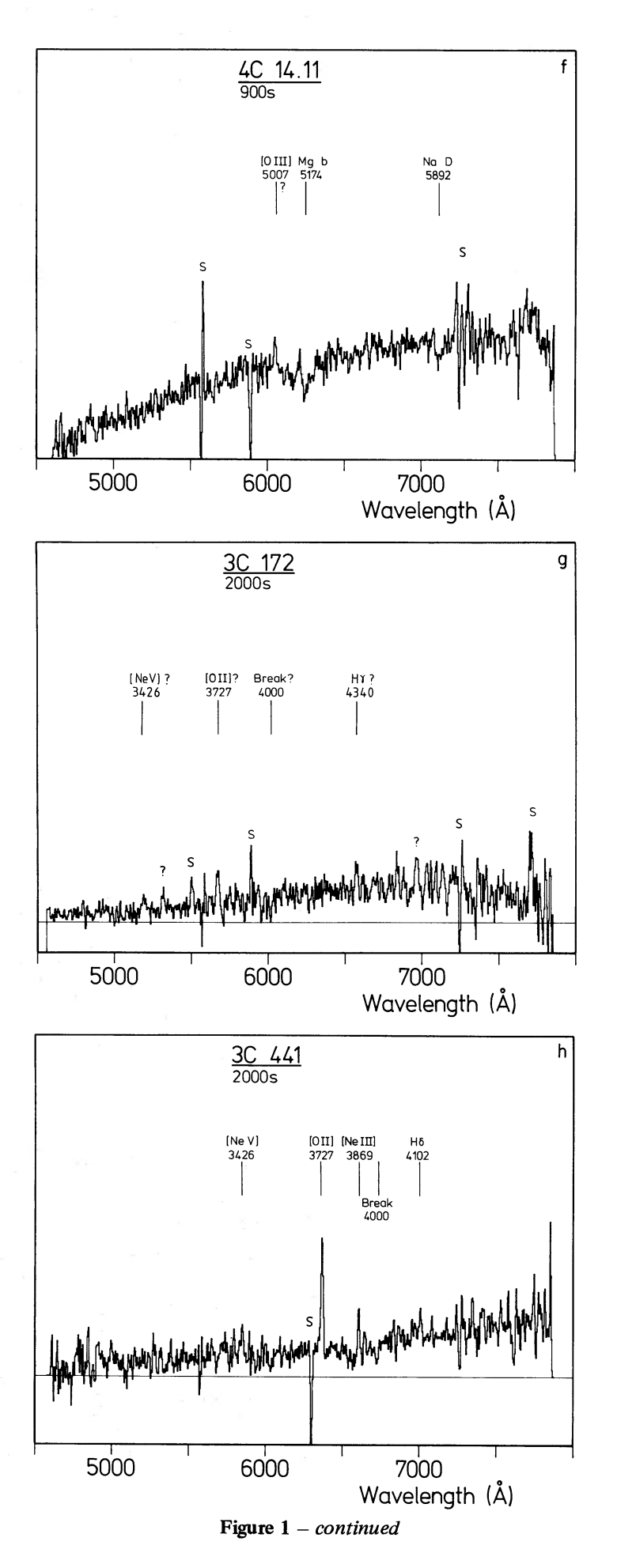


Figure 1 - continued



© Royal Astronomical Society • Provided by the NASA Astrophysics Data System

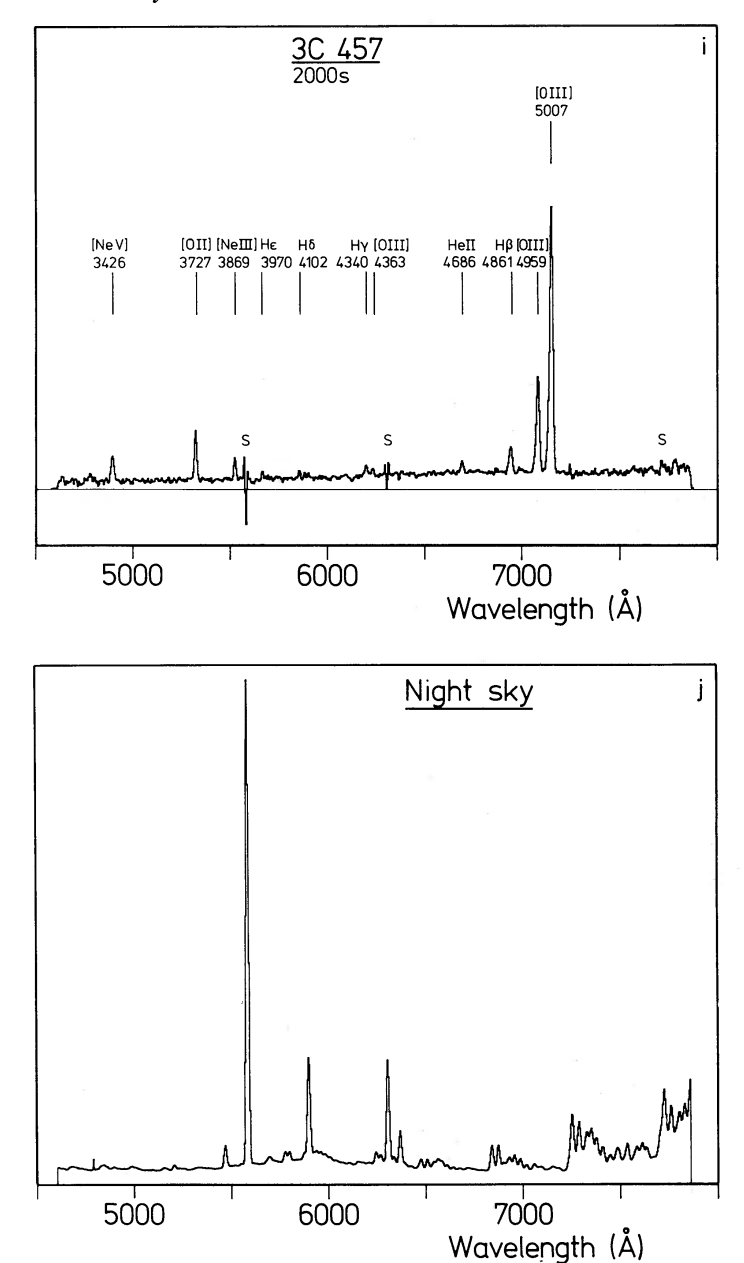


Figure 1 – continued

data over a width of 9 pixels. This permitted more precise calibration of the spectra at the expense of a small reduction in the signal-to-noise ratio in the middle of the spectra. Finally the spectra were smoothed with a Gaussian of standard deviation 4 Å.

Fig. 1 shows the calibrated spectra on a relative energy scale, the small slit width making any absolute calibration uncertain. For multiple exposures the combined spectra were plotted. Imperfectly subtracted night-sky lines (S) and cosmic-ray-event (E) are labelled accordingly. Table 2 lists the identified emission and absorption features for each object, as well as the equivalent width (in the observed frame), the observed wavelength ( $\lambda_{obs}$ ) and the value of the redshift z derived for each line. Estimates of the equivalent width may be in error by up to 20 per cent or more due to uncertainties in the definition of the continuum level. In the final column of the table, absorption lines are indicated by 'a' and uncertain lines by '?'.

Table 2. Identified lines and equivalent widths.

Object		Line	Rest Wavelength	Observed Equivalent	Observed Wavelength	Redshift		
			(A)	Width (A)	λ <sub>obs</sub>	z		
	4C 12.03	G -	4304	6.4	4979.9	0.1570	а	
		[0 III]	4959	2.8	5732.2	0.1559		
		[0 111]	5007	3.6	5786.4	0.1557		
		Mg I b	5174	7.3	5988.5	0.1574	а	
		Na I D	5892	4.3	6815.5	0.1567	а	
		Нα	6563	5.9	7583.5	0.1555		
	3C 14	C III]	1909	39.6	4709.1	1.4668		
		C II]	2326	9.6	5740.3	1.4679		
		[Ne IV]	2424	8.4	5986.9	1.4698		
		Mg II	2799	74.9	6912.1	1.4694		
	3C 22	[Ne IV]	2424	30.0	4694.0	0.9364		
		Mg II	2799	70.5	5424.3	0.9379		
		[Ne V]	3346	15.3	6475.0	0.9351		
		[Ne V]	3426	44.5	6636.7	0.9371		
		[0 II]	3727	200-230	7223.3	0.9381		
		[Ne III]	3869	87.6	7496.0	0.9375		
	3C 41	Mg II	2799	67.9	5019.9	0.7935		
		[0 II]	3727	125.9	6685.9	0.7937		
		[Ne III]	3869	55.5	6946.1	0.7953		
		нδ	4102	30.2	7212.6	0.7600	?	
	3C 65	None						
	4C 14.11	[0 III]	5007	8.2	6046.1	0.2075	?	
		Mg I b	5174	23.6	6235.3	0.2051	a	
		Na I D	5892	6.6	7110.8	0.2068	а	
	3C 172	[Ne V]	3426	~25.0	5186.9	0.5140	?	
		[0 II]	3727	63.5	5667.3	0.5206	?	
		Нγ	4340	~20.0	6576.7	0.5150	?	
	3C 441	[Ne V]	3426	38.3	5842.6	0.7053		
		[0 II]	3727	95.4	6363.1	0.7073		
		[Ne III]	3869	31.8	6602.6	0.7065		
		нδ	4102	16.0	7003.6	0.7074		
	3C 457	[Ne V]	3426	63.7	4888.6	0.4269		
		[O II]	3727	83.9	5318.7	0.4271		
		[Ne III]	3869	37.1	5521.0	0.4270		
		Hε	3970	10.4	5663.0	0.4264		
		Нδ	4102	9.1	5852.0	0.4266		
		Нγ	4340	15.5	6194.5	0.4273		
		[0 III]	4363	9.4	6229.1	0.4277		
		He II	4686	12.1	6688.4	0.4273		
		нв	4861	37.9	6937.2	0.4271		
		[0 III]	4959	133.6	7076.1	0.4269		
		[0 III]	5007	359.6	7144.4	0.4268		

Table 1 lists the resulting emission line and/or absorption line redshifts for each object, based on an equal weighting of the line positions given in Table 2, except for those qualified by '?'. A single correction for galactic rotation has been applied to the redshifts listed in Table 1. Also given is an indication of the ionisation parameter measured by the ratio  $I = f([Ne \ v] \ 3426)/f([O\ II] \ 3727)$ , the approximate wavelength coverage in the object's rest frame and, for reference, the redshift  $(z_{pred})$  predicted by Laing *et al.* (1983) on the basis of the object's optical magnitude and morphological type.

## 3 The spectra

- 4C 12.03 The absorption features in this bright object give an unambiguous redshift of 0.157 consistent with the redshift derived from the weak emission lines.
- Both Kristian, Sandage & Katem (1974) and Riley, Longair & Gunn (1980) noted the stellar appearance of this identification, and the spectrum confirms that it is a quasar. The steep continuum ( $\alpha = 2.4$  where  $f_{\nu} \propto \nu^{-\alpha}$ ) and the equivalent widths of the emission lines are typical of the faint red 3C quasars studied by Smith & Spinrad (1980b).
- The redshift 0.938 of this galaxy is derived from the prominent [Ne v] 3426, [O II] 3727, and [Ne III] 3869 lines. Mg II 2799 is certainly present and, from

- 166 M. A. C. Perryman et al.
  - a comparison of the two individual spectra, both [Ne IV] 2424 and [Ne V] 3346 are likely to be present. The red wing of [Ne III] is possibly blended with He I and H8 at 3889 Å. There is clearly a strong ultraviolet continuum in this galaxy.
- 3C 41 The emission-line redshift of 0.795 is based principally on [O II] 3727 and [Ne III] 3869. The high-excitation line [Ne v] 3426 is weak or absent, giving a limit of l < 0.08.
- 3C 65 This is the faintest object observed in this programme, with r = 23 mag. Although the continuum is clearly detected, there are no recognizable emission or absorption features, and no redshift has been determined.
- 4C 14.11 The redshift of z = 0.206 is based on two absorption features and the possible presence of [O III] 5007.
- A tentative redshift measurement of 0.52 may be made by identifying the most prominent emission feature with [O II] 3727. Other possible weak emission lines at this redshift are [Ne v] 3426 and Hγ 4340, and the 4000 Å feature may also be present. Nevertheless, this redshift is much less certain than the others and should certainly be confirmed.
- 3C 441 The redshift of 0.708 is based on four emission lines. [O II] 3727 is prominent, and the 4000 Å feature can also be identified.
- 3C 457 The spectrum shows a large number of strong emission-lines covering a wide range of ionization potentials, and the ionization parameter is very high (I = 0.75). The redshift is 0.428.

#### 4 Discussion

The successful redshift determinations presented in this paper have significantly reduced the number of 3CR identifications requiring spectroscopic redshift measurement. Of the 53 3CR sources in the statistical sample in the RA range from 0–8 hr, redshifts have now been obtained for all but 3C 65 and 68.2, the latter being an optically empty field (Gunn et al. 1981), although there is still some doubt as to the correctness of one or two of the identifications (e.g. 3C 13). We note the generally good agreement with the predicted redshifts for these objects made by Laing et al. (1983) on the basis of the optical magnitudes of the proposed identifications and an empirical optical Hubble diagram constructed using data on those identifications with measured redshift (see the final column of Table 1).

The fact that we have been successful in obtaining redshifts for galaxies fainter than 20th magnitude is almost entirely due to the presence of strong narrow emission-lines. The presence of strong emission lines considerably reduces the probability that the identification is a chance positional association of a foreground object with the radio source, and hence serves as a useful confirmation of the identification. These probabilities are calculated for all the proposed identifications by Laing *et al.* (1983). Those candidates with strong emission lines (i.e. 3C 14, 22, 41, 441 and 457) must now be secure. We note that the two galaxies for which redshift determination was difficult or impossible (3C 172 and 65 respectively) due to the absence of strong emission lines have the highest probabilities (0.20 and 0.08 respectively) of incorrect identification of the nine objects observed.

In the case of 3C65, [OII] 3727 emission of comparable strength to that found in 3C22, 41 and 441 should have been observable provided the redshift z < 1.2. It may be, however, that the system does not possess a strong narrow-line spectrum. Lilly & Longair (1984) have found a relation between the equivalent width of the [OII] 3727 Å line and the (r-K) optical to infrared colour in the sense that those galaxies with strong [OII] also have the bluest continuum radiation. Their observations suggest that 3C65 has at most a small (r-K) excess and hence we might expect that [OII] may be weak or absent in this object.

The origin of the blue continuum radiation in the high-redshift radio galaxies is of considerable interest. It might be of non-thermal origin but it is more likely that it is the emission from an enhanced population of young stars in these galaxies. In support of this interpretation, a cross-correlation analysis using a standard galaxy spectrum provided confirmation of the emission-line redshift in the case of 3C 41, 172 and 441 by suggesting the presence of an underlying stellar continuum. In addition, a study of the galaxy 3C 352 (redshift z = 0.8) by Lilly, Longair & McLean (1983) showed that there is an excess of radiation in the observed optical B band and that it is likely to be associated with a young stellar population distributed throughout the galaxy. A similar result has been found for a number of other high-redshift galaxies (Lilly & Longair 1984). Such an origin appears to be compatible with the present observations of the strong narrow-line radio galaxies 3C 22, 41 and 441. One test of this hypothesis is straightforward – deep photometric images of these galaxies over a range of optical wavebands should show enhanced emission at the shorter wavelengths over the entire galaxy, as in 3C 252. One interesting aspect of this work and of previous spectral investigations has been the fact that it has generally been possible to distinguish broad-line quasars and narrow-line radio galaxies at large redshifts on the basis of their optical morphology. The objects associated with 3C 22, 41 and 441 are apparently galaxies and this suggests that the rest-frame near-ultraviolet light of these narrow-line galaxies is not dominated by nuclear emission.

## Acknowledgments

We are grateful to the Director of the Kitt Peak National Observatory for the allocation of telescope time, to James De Veny for his assistance at the telescope, and to Jeanette Barnes, Jean Goad and Suzanne Hammond for their assistance in the preliminary reduction of the data. AJBD acknowledges support from Trinity Hall, Cambridge, and SJL acknowledges an SERC Research Studentship.

#### References

De Veny, J., 1982. An Observers Manual for the Cryogenic Camera, Kitt Peak National Observatory.

Goad, J., 1982. A Partial Guide to the IPPS RV Menu, Kitt Peak National Observatory.

Gunn, J. E., Hoessel, J. G., Westphal, J. A., Perryman, M. A. C. & Longair, M. S., 1981. Mon. Not. R. astr. Soc., 194, 111.

Jenkins, C. R., Pooley, G. G. & Riley, J. M., 1977. Mem. R. astr. Soc., 84, 61.

Kristian, J., Sandage, A. & Katem, B., 1974. Astrophys. J., 191, 43.

Laing, R. A., Riley, J. M. & Longair, M. S., 1983. Mon. Not. R. astr. Soc., 204, 151.

Lilly, S. J. & Longair, M. S., 1984. Mon. Not. R. astr. Soc., submitted.

Lilly, S. J., Longair, M. S. & McLean, I. S., 1983. Nature, 301, 488.

Riley, J. M., Longair, M. S. & Gunn, J. E., 1980. Mon. Not. R. astr. Soc., 192, 233.

Scott, P., Hammond, S. & Goad, J., 1982. Long Slit Batch Reduction Manual, Kitt Peak National Observatory.

Smith, H. E. & Spinrad, H., 1980a. Publ. astr. Soc. Pacific, 92, 553.

Smith, H. E. & Spinrad, H., 1980b. Astrophys. J., 236, 419.

Spinrad, H., 1982. Publ. astr. Soc. Pacific, 94, 397.

Spinrad, H., Stauffer, J. & Butcher, H., 1981. Astrophys. J., 244, 382.

Stone, R. P. S., 1977. Astrophys. J., 218, 767.